© 2015. Published by The Company of Biologists Ltd | The Journal of Experimental Biology (2015) 218, 653-663 doi:10.1242/jeb.031203

REVIEW

Bat flight: aerodynamics, kinematics and flight morphology

Anders Hedenström* and L. Christoffer Johansson

ABSTRACT

Bats evolved the ability of powered flight more than 50 million years ago. The modern bat is an efficient flyer and recent research on bat flight has revealed many intriguing facts. By using particle image velocimetry to visualize wake vortices, both the magnitude and time-history of aerodynamic forces can be estimated. At most speeds the downstroke generates both lift and thrust, whereas the function of the upstroke changes with forward flight speed. At hovering and slow speed bats use a leading edge vortex to enhance the lift beyond that allowed by steady aerodynamics and an inverted wing during the upstroke to further aid weight support. The bat wing and its skeleton exhibit many features and control mechanisms that are presumed to improve flight performance. Whereas bats appear aerodynamically less efficient than birds when it comes to cruising flight, they have the edge over birds when it comes to manoeuvring. There is a direct relationship between kinematics and the aerodynamic performance, but there is still a lack of knowledge about how (and if) the bat controls the movements and shape (planform and camber) of the wing. Considering the relatively few bat species whose aerodynamic tracks have been characterized, there is scope for new discoveries and a need to study species representing more extreme positions in the bat morphospace.

KEY WORDS: Bat flight, Aerodynamics, Kinematics, Flight morphology, Adaptation, Energetics

Introduction

There is something about bats that attracts our interest. They are mammals that took to the wing around the KT boundary some 65 million years ago in the ecological turmoil that followed the dramatic environmental changes that drove the dinosaurs to extinction. Thereafter, bats underwent an adaptive radiation that led to early forms, such as *Icaronycterix index* and *Onychonycteris finneyi* (Jepsen, 1970; Springer et al., 2001; Simmons et al., 2008), which looked nearly as modern bats already more than 50 my ago. Today, about every fifth mammal species is a bat and as a group bats are only outnumbered by the rodents. Yet, their nocturnal life-style make them less conspicuous than other animals, and their dark-seeking habits have also been the source of many myths as well as misconceptions about their life. With modern techniques this is rapidly changing (Kunz and Parson, 2009), and research interest on bats is steadily increasing.

The ability of bats to negotiate obstacles in complete darkness was the focus of Lazzaro Spallanzani's experiments in the late 18th century (see Griffin, 1958), but researchers did not discover that bats are able to echolocate by emitting ultrasounds until 1930s (Pierce and Griffin, 1938; Griffin and Galambos, 1941). Flight dynamics was initially studied by means of cinematography (Eisentraut, 1936; Vaughan, 1970) and studies of wingbeat kinematics remained the main approach for aerodynamic analysis until flow visualization techniques were developed (Norberg, 1970, 1976a,b; Aldridge, 1986, 1987; von Helversen, 1986). Wingbeat kinematics and qualitative flow visualization of wake vortices were used to reveal the function of the upstroke during hovering and slow flight versus forward flight (von Helversen, 1986; Rayner et al., 1986), but quantitative aerodynamic studies of bat flight in relation to flight speed had to await the development of modern wind tunnels for animal flight and modern flow visualization techniques. Here, we review what we consider are significant developments regarding the study of bat flight. In doing so, we depart from the traditional order of presenting material by starting with the aerodynamics, followed by flight-related morphology and kinematics of bat flight. The development of knowledge about bat flight, like most other scientific fields, has depended strongly on independent technological advancements that allowed novel observations. This is a continuing process and therefore this paper is best considered as a progress report that hopefully will inspire the development of new research efforts, likely involving new methods, which will extend and deepen our understanding of flight in bats.

Aerodynamics

The flapping motion of the wings and the overall forward speed, U (by definition U=0 m s^{-1} at hovering, and U>0 m s^{-1} at all other flight modes) result in a net speed ($U_{\rm eff}$) of the airflow over the wing at some angle of attack. These properties, together with the morphology e.g. size and cross-sectional shape (thickness, camber) of the wing, determine the overall aerodynamic force. According to fixed wing theory the lift force, L, is:

$$L = \frac{1}{2}\rho S C_{\rm L} U_{\rm eff}^2, \quad (1)$$

where ρ is air density, S is wing surface area, $C_{\rm L}$ is a non-dimensional lift coefficient. Characteristics of the wing, such as thickness, camber and surface texture are included in the lift coefficient, which is a measure of the capacity of the wing to generate lift. In blade-element theory, the total aerodynamic force is obtained by integrating instantaneous forces throughout the whole wing beat as given by expressions such as Eqn 1, where S, $C_{\rm L}$ and $U_{\rm eff}$ vary over time and along the span (e.g. Spedding, 1992). Hence, these models are usually referred to as quasi-steady theories of flight. It should be noted here that time-varying corrections to the quasi-steady theory could be sufficient to accommodate for the occurrence of unsteady lift mechanisms (Usherwood and Ellington 2002, Dickson and Dickinson 2004), although this has not been studied for the highly flexible bat wings.

For a flapping, flexing and elastically deforming wing, the classic quasi-steady blade element analysis is impractical, mainly because it is hard to know how much the parameters in Eqn 1 can be simplified to remain meaningful (Norberg, 1976a, 1976b). An alternative approach is to consider the aerodynamic consequences of the flapping wings by observing the wake vortices, which can be viewed as an aerodynamic imprint representing the force (e.g.

Department of Biology, Lund University, Ecology Building, SE-223 62 Lund, Sweden.

*Author for correspondence (anders.hedenstrom@biol.lu.se)

The Journal of Experimental Biology (2015) 218, 653-663 doi:10.1242/jeb.031203

Anderson, 2011). A fundamental fluid dynamic principle, Kelvin's circulation theorem, states that for a change in aerodynamic force on a wing (can actually be any object), such that will occur during a wing-stroke of a bat, there will be vorticity shed into the wake matching exactly the change in aerodynamic force. In reality, wake vortices roll up in geometric structures, such as undulating loops shed from the wing tips in fast and cruising forward flight, or as closed elliptic loops in slow and hovering flight (e.g. Pennycuick, 1988). These structures can rather conveniently be described geometrically and the integrated vorticity (circulation, Γ) measured and the associated impulse (hence force) can be determined. For a simple power glider with a rectangular flat wake limited by the wingspan ($2b$), a force balancing the weight is obtained when:

$$W = L = \rho U \Gamma 2b. \quad (2)$$

Rearranging Eqn 2 yields the circulation required for weight support as:

$$\Gamma = \frac{L}{\rho U 2b} = \frac{L\bar{c}}{\rho S U}, \quad (3)$$

where S is $2b\bar{c}$, i.e. the wing span multiplied with the mean wing chord $\bar{c}$. It is often convenient to normalize Γ with respect to $U\bar{c}$, so

$$\frac{\Gamma}{U\bar{c}} = \frac{L}{\rho U^2 S} = \frac{L}{2qS}, \quad (4)$$

where q is the dynamic pressure ($=1/2\rho U^2$). By combining Eqns 1 and 4, it is notable that the quantity Γ/U represents half the lift coefficient ($C_L/2$) (Ellington, 1978; Rosén et al., 2007). The maximum steady state lift coefficient of wings at Reynolds number (a measure of the ratio of inertial to viscous forces, $Re=Uc/v$, where v is the kinematic viscosity) relevant to bat flight is ∼1.6 (Ellington, 1984a; Laitone, 1997). The classic approach to diagnose the presence of unsteady effects in flying animals is to perform a quasi-steady aerodynamic calculation, using Eqn 1 with a wing-strip analysis, and if the required lift is not achieved (or calculated $C_L>>1.6$) the analysis implies the presence of unsteady phenomena (Weis-Fogh, 1973, 1975; Ellington, 1984a; Norberg, 1976a,b). There are a number of so-called unsteady aerodynamic phenomena found in animal flight, especially among insects (Sane, 2003), including the delayed stall and a leading edge vortex (LEV), which is a span-wise vortex developed on the top surface of the wing near the leading edge that adds significant amounts of circulation, hence lift of the wing (Ellington et al., 1996). Other so-called unsteady aerodynamic phenomena are the Wagner effect, clap-and-fling, the Kramer effect (due to span-wise rotation of the wing) and wake capture (e.g. Ellington, 1984b; Sane, 2003; Shyy et al., 2010). Irrespective of which aerodynamic mechanism is responsible for the force generated, with the exception of wake capture, the time history and magnitude of the net force is reflected by the vortices and their circulation shed into the wake.

Wakes of real bats

The vortices shed by the wings into the wake of a bat can be measured by a technique called particle image velocimetry (PIV) (Fig. 1). This technique is quite laborious and therefore only a limited number of species have been studied so far (Hedenström et al. 2007, 2009; Johansson et al. 2008; Hubel et al. 2009, 2010, 2012a,b; Muijres et al., 2011a; Spedding and Hedenström, 2009). Even though PIV studies are restricted to wind tunnels, where the animals may have a more controlled flight than in the open, these studies have significantly improved our understanding of the aerodynamics of bat flight. Before going into details we should consider the overall wake structure shed from a bat in steady flight. Wake vortices shed by a Palla's long-tongued bat *Glossophaga soricina*, flying at cruising speed (7 m s^{-1}), are shown in Fig. 2A. Distally, vortex tubes, wingtip vortices, trail the path of the wingtip and shed more or less continuously throughout the wingstroke. A pair of vortices is seen inboard of the tip vortices, of opposite spin to the same-side tip vortex. These vortices are shed from the intersection between the wing and body (wing root) because of a steep gradient in lift force (hence circulation) between the wing and body (usually referred to as 'root vortices'). The root vortices are mainly present during the downstroke (Hedenström et al., 2007; Muijres et al., 2011a; Hubel et al., 2009, 2010, 2012) and in some species also into the upstroke (Muijres et al., 2011a) (Fig. 2A). In addition, towards the end of the upstroke there is a vortex loop shed from the hand wing of each wing (Fig. 2A), with a circulation such that the loop induces an upwash and hence a small negative lift (Hedenström et al., 2007; Johansson et al., 2008; Muijres et al., 2011a; Hubel et al., 2009, 2010, 2012; von Busse et al., 2014). This 'reverse vortex loop' appears to be a feature of the wake unique to bats when flying at

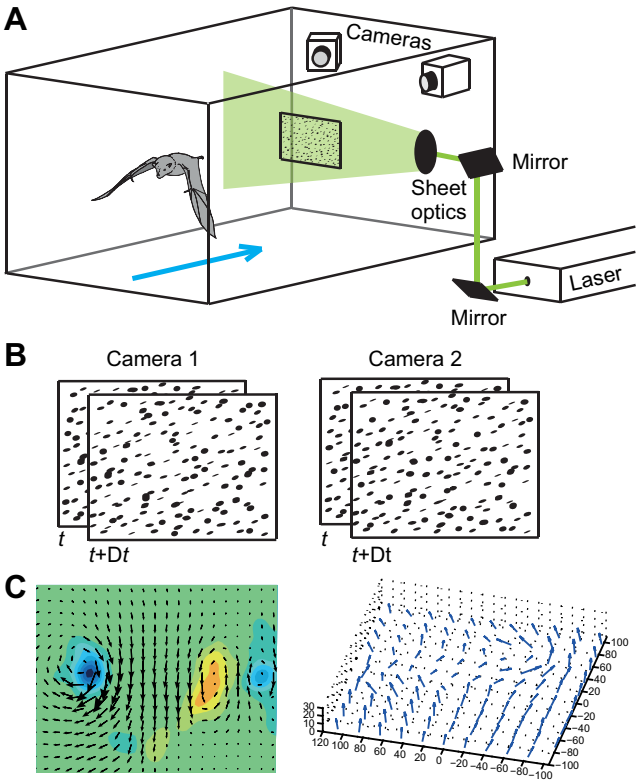

Fig. 1. Particle image velocimetry setup for studying aerodynamics of animal flight. (A) The PIV method uses tracer particles (fog or smoke) suspended in the flow that are illuminated by laser pulses using appropriate mirrors and optics to form a light sheet (or light volume in the case of tomographic PIV). The figure shows a stereo PIV configuration for transverse flow visualization of a bat's wake with two cameras viewing the imaged area from different angles. Blue arrow shows the flow direction in the wind tuunel. (B) Pairs of exposures separated by short interval (the PIV delay, Δt) are the basis for the method. The translation of particles between successive image pairs determines the local flow direction and is used to obtain the velocity field. (C) In stereo PIV, the vector field can be resolved in 3-D. For truly 3-D flow measurement in a volume, a tomographical PIV configuration is required.

The Journal of Experimental Biology (2015) 218, 653-663 doi:10.1242/jeb.031203

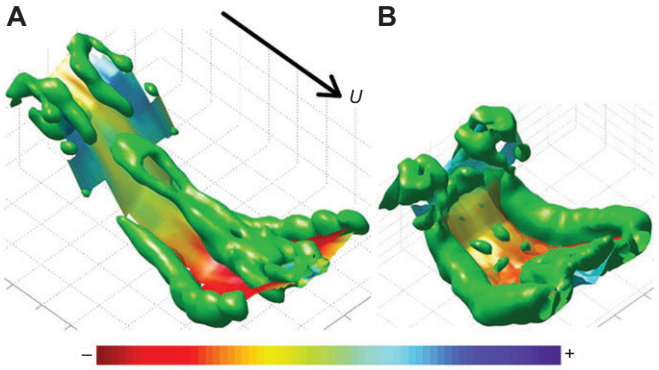

Fig. 2. Vortex wakes generated by Palla's long-tongued bat *Glossophaga soricina*. Bat is flying at (A) 7 m s^{-1} and (B) 4 m s^{-1}. The vortex wake is visualized as iso-surfaces of absolute vorticity $|\omega|$= 125 s^{-1} in both cases. The surface area enclosed by the vortices is colour coded according to vertical induced velocity v, where colour bar range is -1.7 m $s^{-1}<v<1.7$ m s^{-1} in A and -2.6 m $s^{-1}<v<2.6$ m s^{-1} in B. The arrow shows the wind tunnel flow direction (U). Based on Muijres et al. (2011b).

relatively high speed, which to the best of our knowledge has not yet been observed in other animals. When the flight speed is reduced, the reverse vortex loop becomes weaker and disappears altogether at low speed, whereas the tip vortices and root vortices remain the dominant wake features (Fig. 2B) (Muijres et al., 2011a). The actual force production, determined from the strength and size of the wake structures shows that the majority of the force is generated during the downstroke (Fig. 3A) (Muijres et al., 2011a; Hubel et al., 2010, 2012). When separated into weight support and thrust, it is seen that, although the downstroke dominates, thrust and negative lift are generated during the upstroke at high speeds (Fig. 3A; Muijres et al., 2011a,b). Even though it may intuitively seem suboptimal to generate negative lift for a flying animal, optimal wake analysis (Hall and Hall, 1996), suggests that when thrust demands are relatively high it may be optimal to generate thrust during the upstroke, at the cost of negative lift. At the lift to drag ratio (L/D) typical of bats, this may in fact be the case, suggesting that the observed upstroke vortices indicate bats are performing as well as they can considering their force demands (Muijres et al., 2012b). Below a critical speed (~2.5 m s^{-1} in the species studied thus far) the backward speed of the outer wing of the inclined upstroke becomes higher than the forward flight speed (often referred to as a backward 'flick') (Norberg, 1976a,b; Aldridge, 1986, 1987; von Helversen, 1986; Lindhe Norberg and Winter, 2006; Iriarte-Diaz et al., 2011; Wolf et al., 2010; von Busse et al., 2012), with the result that the outer wing generates aerodynamic force mainly perpendicular to the wing path (Hedenström et al., 2007). The hand wing works in an upside-down fashion, and the net force is directed upwards, but mainly forwards (Fig. 4A), which allows the slow flight and hovering kinematic mode unique to bats. At low speeds and hovering, it is often difficult to interpret the wake signatures since wake elements from consecutive wing beats are present in the same PIV plane, and they interact with each other to yield deformed wake structures. However, both transverse wake measurements and measurements near the wings show that the upstroke is aerodynamically active during the upstroke (Fig. 4B; Hedenström et al., 2007; Johansson et al., 2008; Muijres et al., 2014). In Fig. 5, we illustrate how we envisage the direction and relative magnitude of aerodynamic forces from the downstroke and upstroke in relation to forward speed.

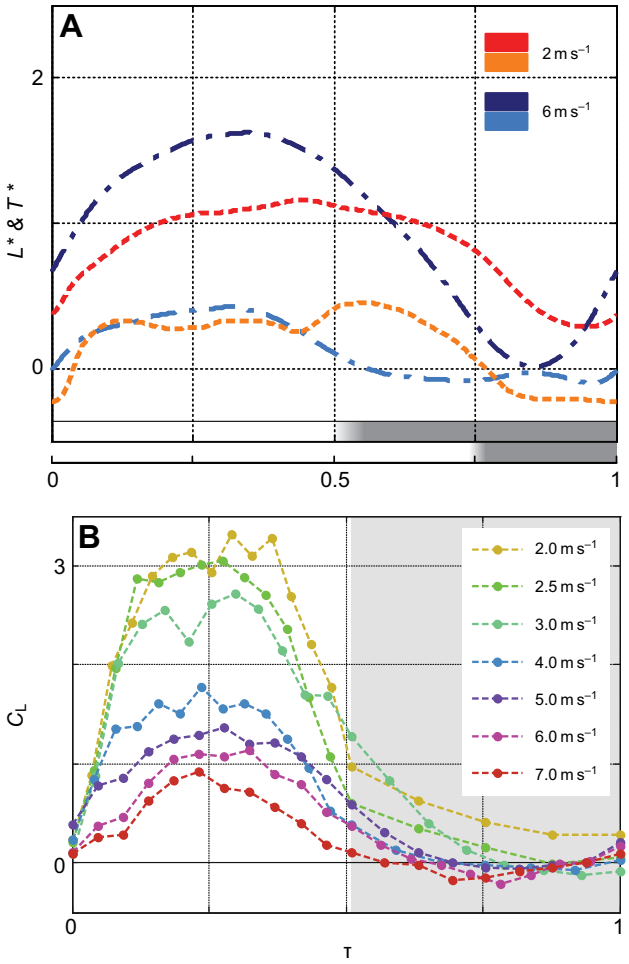

Fig. 3. Force and lift coefficient of lesser short-nosed bat *Leptonycteris yerbabuenae* at different flight speeds during normalized wingbeats ($0<\tau<1$). (A) Normalized lift (L) (dark blue and red) and thrust (T) (light blue and orange). Shaded areas below the graph indicate the upstroke with upper scale for fast (6 m s^{-1}) flight and lower scale for slow (2 m s^{-1}) flight. Redrawn from Muijres et al. (2011a). (B) Lift coefficients (C_L) reach values above maximum steady-state values at low speeds at mid-downstroke. Upstroke is shaded grey. From Muijres et al. (2011b).

Lift and the leading edge vortex

Early calculations of weight support in slow flying bats, based on kinematics and steady state aerodynamics suggested that the required C_L by far exceeded the maximum attainable steady state C_L at hovering and slow forward flight speed. For example, using the strip-analysis based on kinematic data, Norberg (1976b) calculated a lift coefficient up to 6.4 (a conservative estimate was 3.1) in the brown long-eared bat *Plecotus auritus* and concluded that 'non-steady-state aerodynamics must prevail'. Also, the more recent direct measurements of the wake circulation behind bats and Eqn 4 result in a C_L well above the steady state maximum at slow flight speeds (Hedenström et al., 2007; Muijres et al., 2011a; Hubel et al., 2012). In a detailed actuator-disc analysis adapted to bat wake data, Muijres et al. (2011b) calculated C_L based on the downwash throughout the wing-stroke in two bat species. The data for the lesser long-nosed bat *Leptonycteris yerbabuenae* are shown in Fig. 3B, from which it is clear that C_L peaks around the mid-downstroke, with values near 0 (or below at high speed, but >0 at $U<2.5$ m s^{-1}) during the second half of the upstroke. These data also show that the maximum C_L depends on forward flight speed, where $C_L \approx 1.6$ at

The Journal of Experimental Biology (2015) 218, 653-663 doi:10.1242/jeb.031203

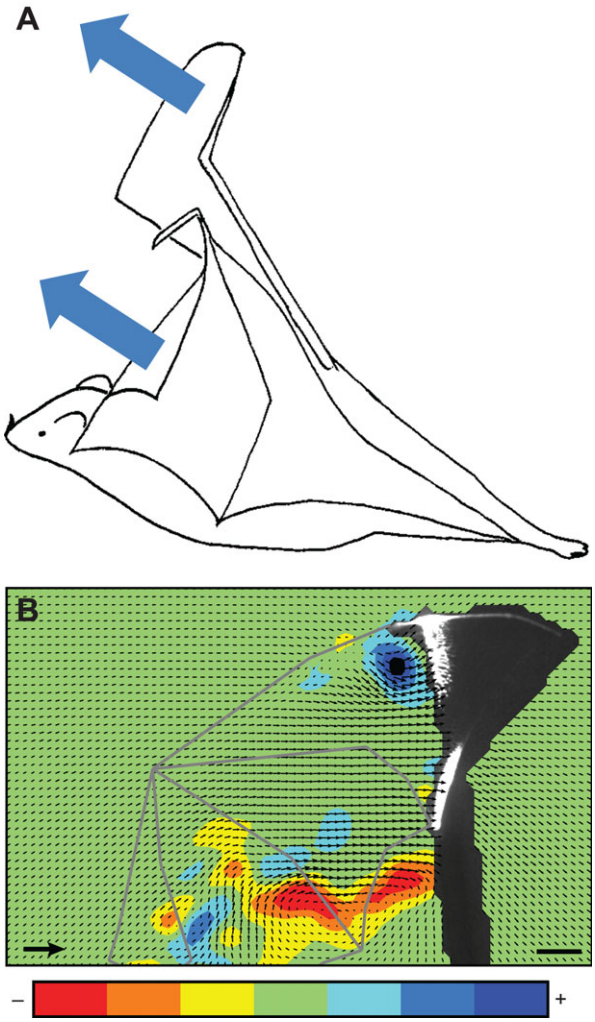

Fig. 4. Aerodynamics of upstroke at slow flight speed. (A) Direction of the aerodynamic force generated during the upstroke in a hovering or slow flying bat. (B) Vector field showing a leading edge vortex on the morphological low side of the wing during the inverted upstroke at low flight speed in *Leptonycteris yerbabuenae*. The scale bar represents 10 mm and the reference vector represents 10 m s^{-1}. From Muijres et al., 2014.

U=4 m s^{-1} and at lower speeds C_L reaches values of 3 or more (Fig. 3B), which is consistent with other studies (e.g. Hubel et al., 2012, see also Table 1). Hence, the values at slow speeds signal the presence of some unsteady aerodynamic mechanism, while this is not required at higher speeds.

The dominating unsteady mechanism used in nature is the dynamic stall and associated LEV, which have been shown for many insects (Ellington et al., 1996; Birch and Dickinson, 2001; Sane, 2003; Johansson et al., 2013), and a few bird species (Muijres et al., 2012a, Warrick et al., 2009, Wolf et al., 2013). In this context, wind tunnel experiments of on-wing flow measurements of slow flying bats have demonstrated the presence of LEVs in the relatively small Palla's long-tongued bats (Fig. 6; Muijres et al., 2008); in slow forward flight (1 m s^{-1}) the LEV contributes up to 40% of the total aerodynamic force (Table 1). Thus far a LEV has been demonstrated also in another species, the lesser long-nosed bat (Table 1; Muijres et al., 2014), but there is nothing extraordinary about the morphology or flight style in these species compared with other species of similar size that are able to fly slowly or hover as part of their feeding strategy. During the upstroke at slow speed, the

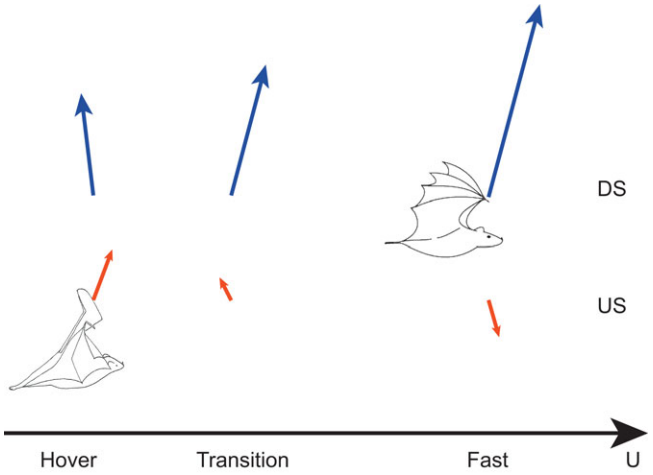

Fig. 5. Schematic illustration of forces generated by the downstroke (DS) and upstroke (US). Forces developing at hover, the transition speed where forward speed and wing speed are similar but have opposite direction, and at fast cruising speed are shown. The arrows show relative magnitude and direction of the aerodynamic forces.

lesser long-nosed bats developed a LEV at the outer wing's morphological ventral side, which because of the backward flick motion acts as aerodynamic up-side of the wing (Fig. 4B; Muijres et al., 2014). Published cases where the lift coefficient has been estimated according to Eqn 4 or blade-element analysis are given in Table 1, indicating that the presence of LEV should be more general among bats during slow flight. In addition, a flapper study, based on the wing shape and kinematics of *Leptonycteris yerbabuenae* has demonstrated that given a high enough angle of attack, LEVs develop above the sharp leading edge wings of bats (Koekkoek et al., 2012). We therefore expect that most, if not all, bat species capable of hovering and slow flight will use LEVs to increase their aerodynamic lift.

Aerodynamic efficiency

A 3-D characterization of the wake allows not only the estimation of lift, but also estimation of the horizontal thrust force and hence drag. In turn, this allows estimation of the important L/D ratio. Muijres et al. (2011a) estimated the maximum effective L/D for flapping flight at 6.9 in *L. yerbabuenae* and 7.5 in *G. soricina*. These values are similar to the maximum L/D of a dog-faced bat *Rousettus aegyptiacus* in gliding flight, estimated at 6.8 in a tilted wind tunnel (Pennycuick, 1971). Although the performance of *L. yerbabuenae* and *G. soricina* is very similar, it turns out that the smaller *G. soricina* has its maximum at a lower flight speed than the larger, migratory *L. yerbabuenae*, suggesting adaptations related to the ecology of the species, where the larger *L. yerbabuenae* commutes over longer distances than *G. soricina* and performs seasonal migrations (Muijres et al., 2011a). Interestingly, flight speed of the minimum angular velocity of the wing, which is directly related to the flight muscle contraction speed and thus the efficiency of the muscles, coincides with the flight speed of maximum L/D (Fig. 7; von Busse et al., 2012). This would suggest that the bats are both aerodynamically and physiologically optimized for the same flight speed.

Another measure of aerodynamic efficiency is the span efficiency (e_i), which measures the ratio of the ideal induced power and the measured induced power (determined by the deviation of the downwash distribution along the wing span from a uniform downwash) (Spedding and McArthur, 2010). Muijres et al.

The Journal of Experimental Biology (2015) 218, 653-663 doi:10.1242/jeb.031203

Table 1. Bat species and number of individuals (*N*) that have been studied and analysed regarding lift coefficient (C_L)

Species	*N*	*M* (kg)	*b* (m)	*S* (m^2)	*Q* (N m^{-2})	AR	FM	*U* (m s^{-1})	Re	C_L	Method	Source
Glossophaga soricina	2	0.011	0.24	0.0091	11.9	6.3	F	1.5	4000	5.97	PIV, Kin	Hedenström et al., 2007
Glossophaga soricina		0.011	0.24	0.0091	11.9		F	7	18,000	0.64		
Glossophaga soricina	3	0.0105	0.242	0.00929	11.2	6.3	F	1	5000	5.4	PIV, Kin	Muijres et al., 2008
Leptonycteris yerbabuenae	2	0.0226	0.329	0.01552	14.2	7.0	F	4	32,000	2.6	PIV	Hedenström et al., 2009
Cynopterus brachyotis	3	0.0307	0.3937	0.0233	13.14	6.7	F	3.4–5.5	16,700–27,000	0.6	PIV, Kin	Hubel et al., 2009
Cynopterus brachyotis	4	0.034	0.347				F	3	-	0.7	PIV, Kin	Hubel et al., 2010
								5	-	0.285		
Plecotus auritus	1	0.009	0.27	0.0123	7.18	5.9	F	0	-	3.1	Kin	Norberg, 1976b
Plecotus auritus	1	0.009	0.27	0.0123	7.18	5.9	F	2.35	-	1.6	Kin	Norberg, 1976a
Rousettus aegyptiacus	1	0.1183	0.554	0.0566	20.5	5.4	G	5.3	32,600	1.5	Kin	Pennycuick, 1971
Rousettus aegyptiacus	1	0.1183	0.461	0.0399	29.1	5.34	G	11	67,900	0.33	Kin	Pennycuick, 1971
Tadarida brasiliensis	5	0.0118	0.26	0.007	16.5	9.8	F	2.8	-	3.94	PIV	Hubel et al., 2012
								8.3	-	0.54	PIV	Hubel et al., 2013

M, mass; *b*, wingspan; *S*, wing area; *Q*, wing loading; AR, aspect ratio; FM, flight mode (F, flapping; G, gliding); *U*, forward airspeed; *Re*, Reynolds number; Method: PIV, particle image velocimetry for flow visualization; Kin, measures derived on the basis of kinematics.

(2011b) found $e_i \approx 0.8$ for both *G. soricina* and *L. yerbabuenae*, with almost no variation across the speed range 2–7 m s^{-1}. This value of e_i refers to the mean span efficiency throughout a wingbeat.

When comparing L/D and e_i with two species of passerine birds, Muijres et al. (2012b) found that birds exhibit higher flight efficiency than bats. The main reason for this is that the bird body generates relatively more lift than the bat body. This could be because the bat is less efficient in generating a downwash than a bird, probably because of its shape and protruding ears.

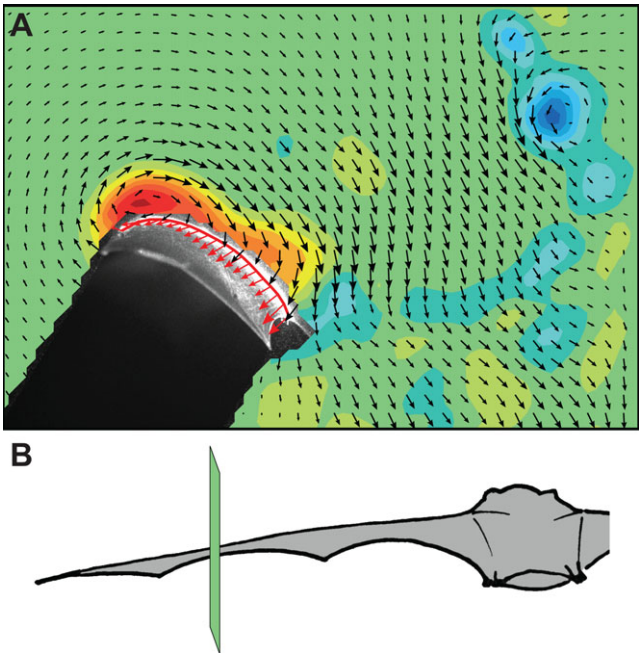

Fig. 6. A leading edge vortex attached to the wing midway through the downstroke of a Palla's long-tongued bat *Glossophaga soricina*. (A) The blue patch in the top right corner is the start vortex shed at the beginning of the downstroke when lift is increasing rapidly. The black arrows show the induced velocity field, whereas red arrows along the wing chord show the velocity of a mid-wing segment. (B) Position along the wingspan of the measurement in A. Based on Muijres et al. (2008).

Functional morphology for bat flight

Wings

Bat wings are unique among extant actively flying animals, formed by a thin skin membrane stretched by elongated arm and hand bones. The wing is divided into sections as defined by the bone elements. The inner wing, proximal to the first and fifth digits, is formed by the propatagium and the plagiopatagium (Fig. 8). The hand wing, the dactylopatagium (d.), is subdivided into d. major, d. medius, d. minus and d. brevis (Fig. 8). Compared with birds and insects, bat wings are relatively compliant and have wider range of possible morphological adjustment, implying an ability to control wing morphology according to the aerodynamic demands. At the same time, the construction implies a number of 'design' problems, such as how to keep the membrane taut to minimize the drag of the wing.

The bat forelimb has elongated bones relative to non-flying mammals, resulting in a large wing area (e.g. Simmons, 1994; Swartz, 1997; Swartz and Middleton, 2008). The humerus and radius have relatively large diameter and thin walls compared with other, similar sized, mammals (Swartz et al., 1992; Swartz, 1997; Swartz and Middleton, 2008), implying an ability to withstand large bending and twisting forces while minimizing the weight (Swartz et al., 1992). The wing bones show a gradient of reduced mineralization from base to tip, which reduces the density of the bone towards the wing tip and makes them more flexible (Norberg, 1970; Papadimitriou et al., 1996; Swartz, 1997; Swartz and Middleton, 2008).

The bones and skin form an intricate unit in the bat wing. The skin is 4–10 times thinner than expected for similar sized mammals and has unique properties among mammals. The skin of the wings shows a strong anisotrophy, with maximum stiffness and strength along the direction of the bones of the digits and with the largest

The Journal of Experimental Biology (2015) 218, 653-663 doi:10.1242/jeb.031203

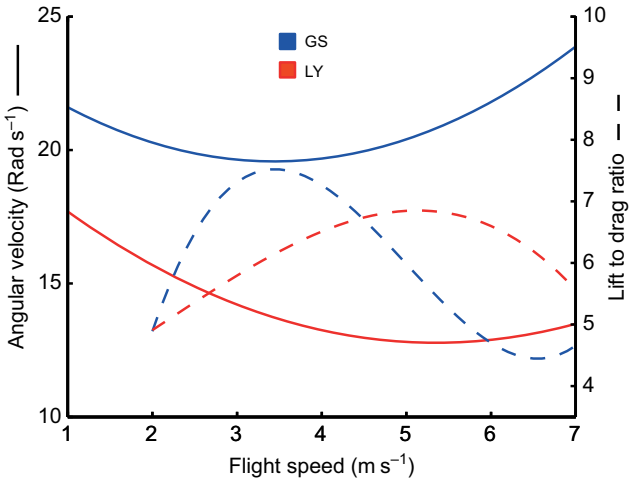

Fig. 7. Comparison of angular velocity of the wing in the stroke plane with lift to drag ratio. Angular velocity (solid lines) and *L*/*D* ratio (dashed lines) in *Leptonycteris yerbabuenae* (LY) and *Glossophaga soricina* (GS). Minimum angular velocity coincides with maximum *L*/*D* in both species, suggesting simultaneous optimization of muscle work and aerodynamic performance. The two species differ in optimal speed, reflecting differences in ecology. Redrawn from von Busse et al., 2012 and Muijres et al., 2011a.

compliance parallel to the trailing edge of the wing (Swartz et al., 1996). These properties are also reflected by in-flight measurements of skin strain in bats (Albertani et al., 2011). It is thought that this arrangement helps reduce shearing forces at the bones and is achieved by a highly structured network of collagen/elastin fibres running parallel to the bones and trailing edge, respectively (Holbrook and Odland, 1978; Vaughan, 1966; Swartz et al., 1996).

Aerodynamic loading of the wing results in a tensioning of the membrane and consequently a force pulling the digits together (Norberg, 1969, 1970), which would result in a bulging membrane. In addition to that, the inner wing is partly folded during the upstroke causing some slackness in the membrane. A slack wing membrane may cause oscillation, similar to a flag, resulting in a substantial increase in the drag (e.g. Alben and Shelley, 2008). We expect the bat to try to avoid a slack membrane and find several features of the wing that may act to reduce or avoid slack. Within the plagiopatagium there are muscles unique to bats that originate on the skeleton and insert in the membrane (Fig. 8) (e.g. MacAlister, 1872; Vaughan, 1959, 1966; Norberg, 1970, 1972b). When these muscles contract, they tension the membrane and the leading and trailing edges. In the plagiopatagium there are also several intramembranous muscles, running parallel to the cord (Fig. 8) (Norberg, 1972b; Swartz et al., 1996). These muscles do not connect to any bone and contraction will mainly tighten the plagiopatagium and reduce the slack of the membrane (Cheney et al., 2014). Along the leading edge of the inner wing, the propatagium, a muscle (m. occipito-pollicalis) runs from the body and inserts on the anterior side of the second metacarpal (Vaughan, 1959; Norberg, 1970, 1972b). Contraction of this muscle will keep the leading edge of the propatagium and the d. brevis stretched.

The trailing edge of the wing is formed by the plagiopatagium, d. major and d. medium (Fig. 8). In all of these sections the trailing edge is concave, causing spreading of the digits to result in an anterio-posterior tensioning of the membrane. In order to maintain an aerodynamically functioning wing, it is important to keep the leading edge of the wing stretched (Norberg, 1969, 1972a). In the inner part of the wing, the leading edge is, as mentioned above, stretched by a muscle running along the leading edge, whereas in the distal part, the second and third digits form the leading edge. The d. minus is kept taut by a mechanism where pulling the second digit forward will automatically result in a tensioning of d. minus, making the leading edge of the wing stiff, which is described in detail by Norberg (1969, 1970, 1972a). A similar mechanism has been suggested for the d. medium between the third and fourth digits (Norberg, 1972a). It is especially difficult to keep the distal-most part of the wing membrane stretched. The second phalange of the third digit is most likely pulled anteriorly by the action of the ligament from the tip of the second digit connecting to the anterior side of the base of the phalange (Fig. 8), but how the third phalange is tensioned is unclear. In addition, these two distal-most bone elements are the least mineralized in the bat wing (Papadimitriou et al., 1996; Swartz and Middleton, 2008). This has been suggested to allow for high levels of bending without failure of these bones when subjected to aerodynamic forces (Papadimitriou et al., 1996). However, kinematic analysis suggests relatively little bending of these bones during flight (von Busse et al., 2012). Unlike the other phalanges, which are laterally compressed, these bones are

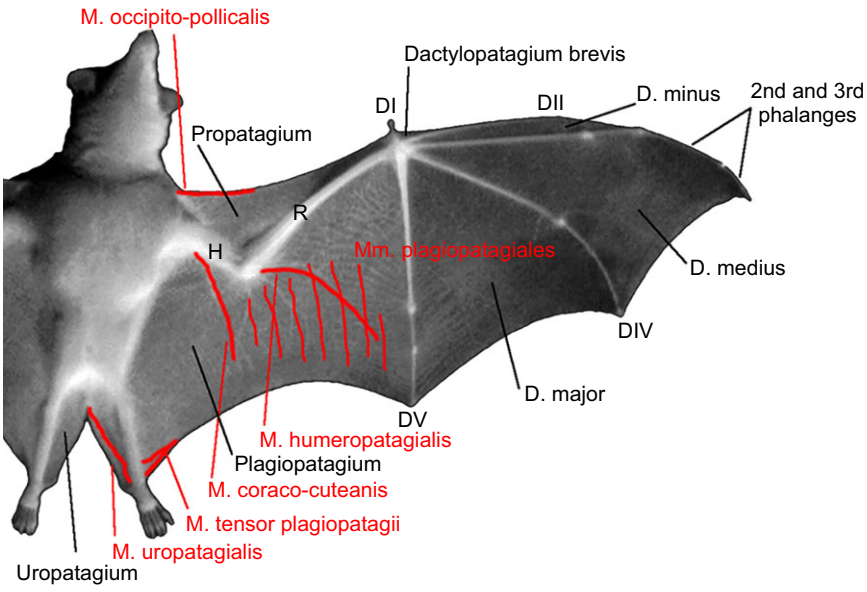

Fig. 8. Morphology of the bat wing. Humerus (H), radius (R), the digits (DI–DV) and the different membranes, propataguim, plagiopatagium, dactylopatagium (d. brevis, d. minus, d. medius, d. major), uropatagium and a number of muscles (red) associated with tensioning of the wing membrane are indicated.

The Journal of Experimental Biology (2015) 218, 653-663 doi:10.1242/jeb.031203

dorso-ventrally flattened or circular in cross section (Vaughan, 1959; Norberg, 1970, 1972b). This suggests that these distal bones are mainly adapted to withstand forces within the plane of the membrane. Interestingly, these bones are responsible for the stretching of the outermost part of the wing membrane, including the trailing edge of the d. medius. It is possible that these bones act as pre-tensioned springs with the main function to keep the membrane and the trailing edge stretched, rather than being selected for compliance due to high aerodynamic forces.

Uropatagium

The shape and size of the uropatagium (Fig. 8), the membrane between the legs, vary considerably among bats (Norberg and Rayner, 1987; Bullen and McKenzie, 2001). In many insectivorous bats the uropatagium has important functions for prey capture, which is reflected by the skin being more resistant to puncture than the wing membrane (Swartz et al., 1996). Any possible aerodynamic function of the uropatagium is not clear at present, but in-flight observations suggest it is partly involved in control of manoeuvring (Bullen and McKenzie, 2001). A control function has also been suggested by force measurements on bat models (Gardiner et al., 2011). The species studied during free flight using PIV so far, have small or even indented 'negative' tail membrane and the wakes have suggested a relatively limited aerodynamic function of the body and tail (Hedenström et al., 2007; Johansson et al., 2008; Hedenström et al., 2009; Hubel et al., 2009; Hubel et al., 2010; Muijres et al., 2011a; Hubel et al., 2012). However, unlike birds where the tail is a separately controlled aerodynamic surface, bat tails are connected to the wings because both attach to the legs. As a result of the function of the legs in controlling the camber (see below) and potentially also the tension of the inner wing, we suspect that the aerodynamic function of the uropatagium could be compromised by the aerodynamics of the wings. We therefore suggest that studying species with different relative sizes of the uropatagium would be of great interest to elucidate the aerodynamic consequences of this membrane.

Ears

Bats have rather large ears because of their echolocating capabilities. This has led to the speculation that the ears could be part of the lift-generating airframe of bats (Vaughan, 1966; Fenton, 1972). However, results of forces generated by modelled bat bodies with large ears have been discouraging in that respect, suggesting that drag is mostly generated when the ears are erected (Gardiner et al., 2008). The ears are in fact similar to concave, forward-facing discs, which are known to generate high drag (Hoerner, 1965). The relatively low aerodynamic lift generated by the body in PIV measurements has also been speculated to be partly due to the ears and nose leaves of bats (Johansson et al., 2010; Muijres et al., 2012b). Based on current evidence we therefore suggest that the ears and their associated aerodynamic costs are structures that bats simply have to live with as a result of their lifestyle. It would therefore be interesting to compare the relative size of ears among insectivorous (highly dependent on echolocation) and frugivorous (less dependent on echolocation) bats to see whether there is selection against the size of ears in bats related to the use of echolocation.

Ecomorphology of bat wings

In bats, as well as in birds and insects, there is a variation in wing morphology associated with general aerodynamic requirements (Fig. 9). For example, long slender wings are highly efficient for transportation flight and large broad wings for high manoeuvrability (Norberg and Rayner, 1987) (Fig. 9). However, the morphospace occupied by bats is smaller than that of birds and insects, suggesting a smaller variation in wing morphology among bats (Rayner, 1988; McGowan and Dyke, 2007). The variation in wing morphology is correlated with ecology and, in general, bats are considered to follow the same pattern as birds, i.e. large, long and slender wings associated with slow cruising flight and short, broad wings associated with high manoeuvrability. On average, bats have lower wing loadings than birds, indicative of a greater manoeuvring capacity (Norberg, 1981; Rayner, 1988). However, the recent wake studies of bats (Hedenström et al., 2007; Muijres et al., 2011a,b, 2012b; Hubel et al., 2009, 2010, 2012) suggest that calculating the wing loading in birds and bats the same way may not be appropriate because the body of bats appears to be relatively aerodynamically inactive compared with birds. Establishing a proper measure of comparison is thus a challenge for future comparative studies. Be that as it may, it would be of great interest to conduct a direct comparison of manoeuvrability between similar sized bats and birds using the same experimental assay.

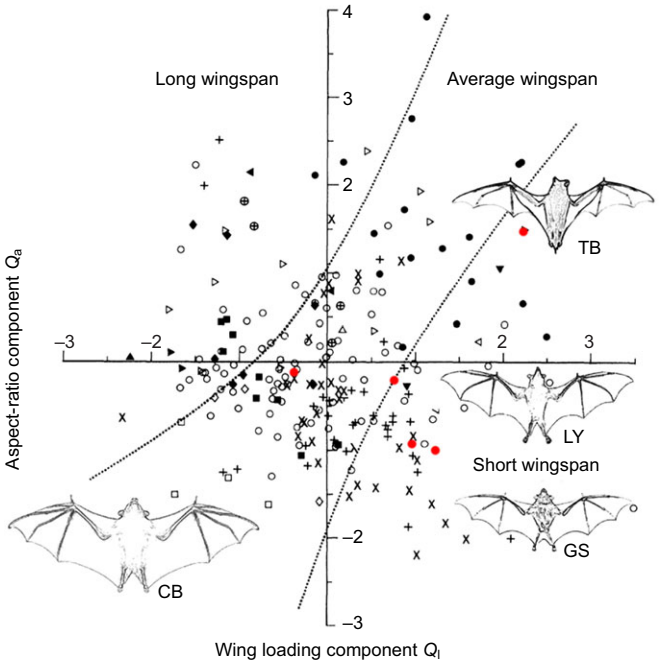

Fig. 9. Bat morphospace expressed with principal component analysis. The horizontal axis represents wing loading and the vertical axis, aspect ratio. From Norberg and Rayner (1987). Silhouettes of species studied using PIV are shown and their position in the figure is indicated in red. TB, *Tadarida brasiliensis*; LY, *Leptonycteris yerbabuenae*; GS, *Glossophaga soricina*; CB, *Cynopterus brachyotis*.

Kinematics

The aerodynamics of flight is controlled by the wing morphology and the kinematics of the animal. Because of the unique morphology of the bat wing compared with the wings of other extant fliers, bats have higher degrees of freedom when it comes to the control of kinematics. As seen above (Eqn 1), the forces generated by a wing are determined by the speed of the wing relative to the air, the wing area and the lift-generating ability of the wing, i.e. the lift coefficient. Bats control all these aspects throughout a wingbeat and across flight speeds.

A change in flight speed is expected to result in changes in kinematic parameters to optimize performance and to be able to

The Journal of Experimental Biology (2015) 218, 653-663 doi:10.1242/jeb.031203

generate enough forces to allow for stable flight. Many of the changes are found in a wide range of species and conform to general expectations for flapping flight. Among variables related to the velocity of the air meeting the wing (U_{eff}, Eqn 1), we find that wing beat frequency decreases (Schnitzler, 1971; Norberg, 1976a; Aldridge, 1986; Lindhe Norberg and Winter, 2006; Riskin et al., 2010; Wolf et al., 2010; Hubel et al., 2012), stroke plane angle increases (becomes more vertical) (Wolf et al., 2010; Lindhe Norberg and Winter, 2006; Hubel et al., 2010; Aldridge, 1986; Riskin et al., 2010; but see Hubel et al., 2012 for contrasting results) and Strouhal number ($St=fA/U_{\infty}$, where f is wingbeat frequency, A is peak–peak amplitude of the wing stroke and U_{∞} is forward airspeed) decreases with increasing flight speed in both micro- and megachiropterans (Wolf et al., 2010; von Busse et al., 2012; Lindhe Norberg and Winter, 2006). The flapping frequency is also expected to decrease with increasing size (Pennycuick, 2008; Bullen and McKenzie, 2002), which is indeed found in comparative data (Bullen and McKenzie, 2002; Riskin et al., 2010; Lindhe-Norberg and Norberg, 2012).

The second factor used for controlling the forces generated is the wing area. With increasing speed, the demands on wing area to generate the same lift are reduced and bats have been shown to reduce the wing area during the downstroke with increasing flight speed (von Busse et al., 2012; Hubel et al., 2010; Hubel, 2012). Several studies have shown a reduction of the wing area during the upstroke, which bats have in common with birds (Wolf et al., 2010; von Busse et al., 2012; Tobalske et al., 2007; Norberg, 1976a). However, the reason for this behaviour is not clear; it was originally suggested as a means to generate a net thrust from a flapping wing with constant circulation (e.g. Pennycuick, 1989), but could also be a way of reducing the inertial cost of the wingbeat (Riskin et al., 2012). Modelling suggests that the wing folding may reduce the inertial cost by as much as 35% in bats, compared with holding wings fully outstretched (Riskin et al., 2012), although this ignores the potential for using aerodynamic forces to move the wing during the upstroke. However, reducing the wing area may also reduce the profile drag of the wing. Optimal wake models (Hall and Hall, 1996; Salehipour and Willis, 2013) often predict a rather unloaded upstroke in which case a reduction of the area of the wing would have little influence on the lift generated, but will reduce the profile drag. The reduction in wing area during the upstroke is correlated with the commonly measured span ratio (the ratio between the horizontally projected span during the upstroke and downstroke). The span ratio is almost constant across speed in bats, with a potential weak negative trend at higher flight speeds (Lindhe Norberg and Winter, 2006; Wolf et al., 2010; Hubel et al., 2010; Hubel et al., 2012). However, although the trend in span ratio is the same across bat species, how this is achieved differs between the pteropodid and microchiropteran species studied. The microchiropteran species keep the handwing taut during the upstroke, whereas wing area and span ratio are mainly controlled by the armwing (Norberg, 1976a; Aldridge, 1986; Wolf et al., 2010; von Busse et al., 2012; Hubel et al., 2012). Pteropodid species, on the other hand, perform a complex retraction of the wing, which involves bending of the digits (Norberg, 1972b; Hubel et al., 2009). Despite this difference in wing kinematics during the upstroke, all bat species studied thus far produce an inversed vortex, indicative of thrust and the production of negative lift, at the end of the upstroke (Hedenström et al., 2007; Hedenström et al., 2009; Hubel et al., 2009; Hubel et al., 2012).

In addition, kinematic factors directly associated with changes in the lift coefficient (Wolf et al., 2010), i.e. angle of attack and camber decrease with increasing flight speed (Wolf et al., 2010; von Busse et al., 2012; Riskin et al., 2010; Hubel et al., 2012). This is probably a consequence of the lower efficiency from operating at high C_L due to associated high drag, whereas the higher speed allows for adequate force production at a lower C_L because lift is related to speed squared across the wing (Eqn 1). In general, bats are able to operate at angles of attack higher than expected for steady wings at relevant *Re*. Steady aircraft airfoils show stall and loss of lift above an angle of attack of about 15 deg (Laitone, 1997), whereas the bats may operate at mean downstroke angles of attack well above these values (Aldridge, 1986; Norberg, 1976a; Riskin et al., 2010; Wolf et al., 2010, von Busse et al., 2012, Hubel et al., 2010, 2012) without apparent loss of lift (Wolf et al., 2010). This suggests that bats may also control the lift throughout the downstroke at these high angles of attack. The highest angle of attack is associated with low flight speeds and consequently the use of LEVs (Muijres et al., 2008; Muijres et al., 2014), which would explain this ability in bats. However, it remains to be shown whether the stability of a LEV is due to active control rather than merely a consequence of a high angle of attack and short translation of the wing.

One of the aerodynamically important morphological parameters of the wing that may be adjusted by bats is camber (Pennycuick, 1973), which partly controls the lift coefficient of the wing (Anderson, 2011; Laitone, 1997; Pelletier and Mueller, 2000) and may control LEV stability (Harbig et al., 2013). Bat wings are capable of larger changes in camber than other extant flying taxa because of the many degrees of freedom for morphing the wing. The camber of the wing has been correlated with increased circulation in the wake showing the ability of the bats to use camber to control the forces generated (Wolf et al., 2010). Several different mechanisms have been suggested to be responsible for changes in camber. Bending of the fifth digit (Vaughan, 1959; Norberg, 1972a) is the most obvious one and kinematic analyses suggest that camber is adjusted mainly by bending at the metacarpal–phalangeal joint (von Busse et al., 2012). Camber of the innermost part of the wing may be achieved by deflection of the legs (Vaughan, 1959, 1966), which is supported by kinematic analyses (Norberg, 1976a; von Busse et al., 2012). Along the leading edge of the wing the propatagium, d. brevis and d. minus (Fig. 8) have been suggested to function as a leading edge flap, capable of adjusting the camber of the wing as well as the curvature of the leading edge (Vaughan, 1959; Norberg, 1990). The propatagium and d. brevis are connected to the thumb in some species (e.g. *G. soricina*) and deflection of the thumb will increase the camber of the inner wing. Deflection of the d. minus is controlled by the second digit and has been found to vary continuously throughout the wingbeat (von Busse et al., 2012), resulting in a change in camber. The above-described mechanisms illustrate the control potential of the bat wing, but also indicate physiological costs, due to muscle contraction, associated with keeping the wing a flexible and efficient aerodynamic surface. In order to actively adjust the wing properties, by bending joints and contracting membrane muscles, to current aerodynamic conditions, the bat needs information about the flow over the wing. Recent exciting results have shown that sensory hairs on the wings may provide this information to the bat (Sterbing-D'Angelo et al., 2011; Chadha et al., 2011) and further analysis of the resolution of the information and the control responses are called for.

Because bat wing morphology is so complex, it is easy to imagine a multitude of different responses to a change in, for example, flight speed or loading, resulting in the same output. In fact, many recent 3-D kinematic studies have found individual differences in the response to changes in speed and loading (Wolf et al., 2010; von Busse et al., 2012; Iriarte-Diaz et al., 2012; Hubel et al., 2010),

suggesting different and idiosyncratic strategies in how to deal with changes in the required output. Investigation of the consequences of such different strategies on the power requirements for flight and aerodynamic control would be a natural next step to increase our understanding of bat flight.

Energetics and flight performance

The power required for flight according to flight mechanical theory follows a U-shaped curve when plotted against airspeed (e.g. Pennycuick, 2008; Hedenström et al., 2009). Strictly, this theory refers to mechanical power output, which is notoriously hard to measure and therefore such data are lacking (but see von Busse et al., 2014 for a recent attempt to do so based on the energy added to the wake). Instead, researchers measure flight metabolic rate or power input, which should reflect the mechanical power–speed relationship if the energy conversion efficiency is constant or nearly so across the speed range. Using a respirometry mask attached to the animal flying in a wind tunnel, a U-shaped power curve was obtained in four species of fruit bats (Thomas, 1975; Carpenter, 1985). More recently, using ^{13}C-labeled sodium bicarbonate, a U-shaped relationship between flight metabolic rate and airspeed was also found in the medium-sized bat *Carollia perspicillata* (average mass 18 g) (von Busse et al., 2013).

The minimum power speed (U_{mp}) and the maximum range speed (U_{mr}) are two characteristic speeds of adaptive importance (Hedenström, 2009). For an ideal bird (*sensu* Pennycuick, 1975), also applicable to a bat, U_{mr} is 1.32 times U_{mp}. From the empirically measured power curve in *C. perspicillata* (von Busse et al., 2013), we estimated U_{mp} as 3.9 m s^{-1} and U_{mr} as 5.2 m s^{-1}, which comes very close to the expected difference between these two characteristic speeds. Bats should select airspeed according to ecological context, for example, when searching for food (U_{mp}) versus commuting or migrating (U_{mr}). That they actually do so has been shown for *Pipistrellus kuhlii*, which flew relatively slowly when searching for food and faster when commuting (Grodzinski et al., 2009). However, whether bats adjust their flight speeds in different ecological situations according to predictions from flight mechanical theory and optimality models (Hedenström, 2009) still remains uncharted territory.

Future directions

The application of the PIV technique to bat flight has revealed a number of new insights, including: (1) bat wakes are more complex than those of birds; (2) the aerodynamic function of the upstroke has been clarified; (3) the lift coefficient during the course of the wingbeat has been quantified; (4) aerodynamic efficiency is lower than in birds; and (5) LEVs are used during both downstroke and upstroke in slow flight. Now that PIV has been applied to a few bat species we may ask whether there are aerodynamic features unique to bats? One such candidate are the vortices shed at the end of the upstroke at relatively high forward speed that are associated with generation of negative lift, which have been observed in all bat species studied thus far. Such vortices arise mainly as a consequence of generating thrust during the upstroke (Hall and Hall, 1996), and although not (yet) observed in other animals, we expect such a wake signature in other flyers operating at similar L/D ratios as bats. It should be noted that aerodynamic studies do not cover the entire morphospace of bats (see Fig. 9), with data still lacking from the extreme ends of the distribution. Future studies should therefore focus on bat species with such morphologies.

Another feature, although not unique to bats, is the use of LEVs to enhance lift, which has been demonstrated in two relatively small species and only at slow speeds (Muijres et al., 2008, 2014). If and how bats actively control the strength of the LEV to prevent it from shedding are still not known. Also, can bats use LEVs when executing fast-turning flight manoeuvres, when a high lift coefficient is also required?

Although initial attempts to correlate the kinematics of bat flight with the quantitative wake measurements are promising (Wolf et al., 2010), understanding how bats control the aerodynamics through changes in kinematics remains a major future challenge. The many degrees of freedom available for bats when controlling their wings (e.g. von Busse et al., 2012) also suggests that the effect of individual strategies for obtaining the same output (e.g. Iriarte-Diaz et al., 2012) will make the effort of understanding aerodynamic control in bats even more challenging. Technical development in the field of computational fluid dynamics and robotics may provide novel insights about the aerodynamic control of bat flight. However, despite the latest developments, the complexity of the bat wing remains a substantial challenge for these techniques (Colorado et al., 2012; Viswanath et al., 2014; Bahlman et al., 2014). Further to this, understanding how bats respond to sensory input about their environment, such as obstacles or flying prey, to execute appropriate kinematic and aerodynamic output will require new experimental approaches. Do the airflow-sensitive hairs on the wings (Sterbing-D'Angelo et al., 2011) play a role in this? There are plenty of challenges left concerning bat flight to keep researchers busy for many years and we can look forward to an exciting future.

Competing interests

The authors declare no competing or financial interests.

Author contributions

Both authors conceived the ideas and wrote the manuscript.

Funding

This research received support from the Knut and Alice Wallenberg foundation to A.H., from the Swedish Research Council to A.H. and L.C.J., the Crafoord foundation to L.C.J. and from the Centre for Animal Movement Research (CAnMove) financed by a Linnaeus grant (349-2007-8690) from the Swedish Research Council and Lund University.

References

Alben, S. and Shelley, M. J. (2008). Flapping states of a flag in an inviscid fluid: bistability and the transition to chaos. *Phys. Rev. Lett.* **100**, 074301.

Albertani, R., Hubel, T., Swartz, S. M., Breuer, K. S. and Evers, J. (2011). In-flight wing-membrane strain measurements on bats. In *Experimental and Applied Mechanics,* Vol. 6 (ed. T. Proulx), pp. 437-445. New York, NY: Springer.

Aldridge, H. D. (1986). Kinematics and aerodynamics of the greater horseshoe bat, *Rhinolophus ferrumequinum*, in horizontal flight at various flight speeds. *J. Exp. Biol.* **126**, 479-497.

Aldridge, H. D. (1987). Body acceleration during the wingbeat in six bat species: the function of the upstroke in thrust generation. *J. Exp. Biol.* **130**, 275-293.

Anderson, J. D. (2011). *Fundamentals of Aerodynamics*. New York, NY: McGraw-Hill.

Bahlman, J. W., Swartz, S. M. and Breuer, K. S. (2014). How wing kinematics affect power requirements and aerodynamic force production in a robotic bat wing. *Bioinspir. Biomim.* **9**, 025008.

Birch, J. M. and Dickinson, M. H. (2001). Spanwise flow and the attachment of the leading-edge vortex on insect wings. *Nature* **412**, 729-733.

Bullen, R. and McKenzie, N. L. (2001). Bat airframe design: flight performance, stability and control in relation to foraging ecology. *Aust. J. Zool.* **49**, 235-261.

Bullen, R. D. and McKenzie, N. L. (2002). Scaling bat wingbeat frequency and amplitude. *J. Exp. Biol.* **205**, 2615-2626.

Carpenter, R. E. (1985). Flight physiology of flying foxes, *Pteropus poliocephalus*. *J. Exp. Biol.* **114**, 619-647.

Chadha, M., Moss, C. F. and Sterbing-D'Angelo, S. J. (2011). Organization of the primary somatosensory cortex and wing representation in the Big Brown Bat, *Eptesicus fuscus*. *J. Comp. Physiol. A* **197**, 89-96.

Cheney, J. A., Konow, N., Middleton, K. M., Breuer, K. S., Roberts, T. J., Giblin, E. L. and Swartz, S. M. (2014). Membrane muscle function in the compliant wings of bats. *Bioinspir. Biomim.* **9**, 025007.

Colorado, J., Barrientos, A., Rossi, C., Bahlman, J. W. and Breuer, K. S. (2012). Biomechanics of smart wings in a bat robot: morphing wings using SMA actuators. *Bioinspir. Biomim.* **7**, 036006.
Dickson, W. B. and Dickinson, M. H. (2004). The effect of advance ratio on the aerodynamics of revolving wings. *J. Exp. Biol.* **207**, 4269-4281.
Eisentraut, M. (1936). Beitrag zur mechanik des fledermausfluges. *Z. Wiss. Zool.* **148**, 159-188.
Ellington, C. P. (1978). The aerodynamics of normal hovering: three approaches. In *Comparative Physiology: Water, Ions and Fluid Mechanics* (ed. K. Schmidt-Nielsen, L. Bolis and S. H. P. Maddrell), pp. 327-345. Cambridge: Cambridge University Press.
Ellington, C. P. (1984a). The aerodynamics of hovering insect flight. I. The quasi-steady analysis. *Philos. Trans. R. Soc. B* **305**, 1-15.
Ellington, C. P. (1984b). The aerodynamics of hovering insect flight. IV. Aerodynamic mechanisms. *Philos. Trans. R. Soc. B* **305**, 79-113.
Ellington, C. P., van den Berg, C., Willmott, A. P. and Thomas, A. L. R. (1996). Leading-edge vortices in insect flight. *Nature* **384**, 626-630.
Fenton, M. B. (1972). The structure of aerial-feeding bat faunas as indicated by ears and wing elements. *Can. J. Zool.* **50**, 287-296.
Gardiner, J. D., Dimitriadis, G., Sellers, W. I. and Codd, J. R. (2008). The aerodynamics of big ears in the brown long-eared bat *Plecotus auritus*. *Acta Chiropt.* **10**, 313-321.
Gardiner, J. D., Dimitriadis, G., Codd, J. R. and Nudds, R. L. (2011). A potential role for bat tail membranes in flight control. *PLoS ONE* **6**, e18214.
Griffin, D. R. (1958). *Listening in the Dark. The Acoustic Orientation of Bats and Men.* New Haven, CT: Yale University Press.
Griffin, D. R. and Galambos, R. (1941). The sensory basis of obstacle avoidance by flying bats. *J. Exp. Zool.* **86**, 481-506.
Grodzinski, U., Spiegel, O., Korine, C. and Holderied, M. W. (2009). Context-dependent flight speed: evidence for energetically optimal flight speed in the bat *Pipistrellus kuhlii*? *J. Anim. Ecol.* **78**, 540-548.
Hall, K. C. and Hall, S. R. (1996). Minimum induced power requirements for flapping flight. *J. Fluid Mech.* **323**, 285-315.
Harbig, R. R., Sheridan, J. and Thompson, M. C. (2013). Relationship between aerodynamic forces, flow structures and wing camber for rotating insect wing planforms. *J. Fluid Mech.* **730**, 52-75.
Hedenström, A. (2009). Optimal migration strategies in bats. *J. Mammal.* **90**, 1298-1309.
Hedenström, A., Johansson, L. C., Wolf, M., von Busse, R., Winter, Y. and Spedding, G. R. (2007). Bat flight generates complex aerodynamic tracks. *Science* **316**, 894-897.
Hedenström, A., Johansson, L. C. and Spedding, G. R. (2009). Bird or bat: comparing airframe design and flight performance. *Bioinspir. Biomim.* **4**, 015001.
Hoerner, S. F. (1965). *Fluid-Dynamic Drag*. Bricktown, NJ: Hoerner Fluid Dynamics.
Holbrook, K. A. and Odland, G. F. (1978). A collagen and elastic network in the wing of the bat. *J. Anat.* **126**, 21-36.
Hubel, T. Y., Hristov, N. I., Swartz, S. M. and Breuer, K. S. (2009). Time-resolved wake structure and kinematics of bat flight. *Exp. Fluids* **46**, 933-943.
Hubel, T. Y., Riskin, D. K., Swartz, S. M. and Breuer, K. S. (2010). Wake structure and wing kinematics: the flight of the lesser dog-faced fruit bat, *Cynopterus brachyotis*. *J. Exp. Biol.* **213**, 3427-3440.
Hubel, T. Y., Hristov, N. I., Swartz, S. M. and Breuer, K. S. (2012). Changes in kinematics and aerodynamics over a range of speeds in *Tadarida brasiliensis*, the Brazilian free-tailed bat. *J. R. Soc. Interface* **9**, 1120-1130.
Iriarte-Diaz, J., Riskin, D. K., Willis, D. J., Breuer, K. S. and Swartz, S. M. (2011). Whole-body kinematics of a fruit bat reveal the influence of wing inertia on body accelerations. *J. Exp. Biol.* **214**, 1546-1553.
Iriarte-Diaz, J., Riskin, D. K., Breuer, K. S. and Swartz, S. M. (2012). Kinematic plasticity during flight in fruit bats: individual variability in response to loading. *PLoS ONE* **7**, e36665.
Jepsen, G. L. (1970). Bat origins and evolution. In *Biology of Bats*, Vol. 1 (ed. W. A. Wimsatt), pp. 1-64. New York, NY: Academic Press.
Johansson, L. C., Wolf, M., von Busse, R., Winter, Y., Spedding, G. R. and Hedenström, A. (2008). The near and far wake of Pallas' long tongued bat (*Glossophaga soricina*). *J. Exp. Biol.* **211**, 2909-2918.
Johansson, L. C., Wolf, M. and Hedenström, A. (2010). A quantitative comparison of bird and bat wakes. *J. R. Soc. Interface* **7**, 61-66.
Johansson, L. C., Engel, S., Kelber, A., Heerenbrink, M. K. and Hedenström, A. (2013). Multiple leading edge vortices of unexpected strength in freely flying hawkmoth. *Sci. Rep.* **3**, 3264.
Koekkoek, G., Muijres, F. T., Johansson, L. C., Stuiver, M., van Oudheusden, B. W. and Hedenström, A. (2012). Stroke plane angle controls leading edge vortex in a bat-inspired flapper. *C. R. Acad. Sci. IIb Mec.* **340**, 95-106.
Kunz, T. H. and Parsons, S. (ed.). (2009). *Ecological and Behavioral Methods for the Study of Bats*, 2nd edn. Baltimore, MD, USA: Johns Hopkins University Press.
Laitone, E. V. (1997). Wind tunnel tests of wings at Reynold numbers below 70 000. *Exp. Fluids* **23**, 405-409.
Lindhe Norberg, U. M. and Winter, Y. (2006). Wing beat kinematics of a nectar-feeding bat, Glossophaga soricina, flying at different flight speeds and Strouhal numbers. *J. Exp. Biol.* **209**, 3887-3897.
Lindhe Norberg, U. M. and Norberg, R. Å. (2012). Scaling of wingbeat frequency with body mass in bats and limits to maximum bat size. *J. Exp. Biol.* **215**, 711-722.
MacAlister, A. (1872). The myology of the cheiroptera. *Philos. Trans. R. Soc. London* **162**, 125-171.
McGowan, A. J. and Dyke, G. J. (2007). A morphospace-based test for competitive exclusion among flying vertebrates: did birds, bats and pterosaurs get in each other's space? *J. Evol. Biol.* **20**, 1230-1236.
Muijres, F. T., Johansson, L. C., Barfield, R., Wolf, M., Spedding, G. R. and Hedenström, A. (2008). Leading-edge vortex improves lift in slow-flying bats. *Science* **319**, 1250-1253.
Muijres, F. T., Johansson, L. C., Winter, Y. and Hedenström, A. (2011a). Comparative aerodynamic performance of flapping flight in two bat species using time-resolved wake visualization. *J. R. Soc. Interface* **8**, 1418-1428.
Muijres, F. T., Spedding, G. R., Winter, Y. and Hedenström, A. (2011b). Actuator disk model and span efficiency of flapping flight in bats based on time-resolved PIV measurements. *Exp. Fluids* **51**, 511-525.
Muijres, F. T., Johansson, L. C. and Hedenström, A. (2012a). Leading edge vortex in a slow-flying passerine. *Biol. Lett.* **8**, 554-557.
Muijres, F. T., Johansson, L. C., Bowlin, M. S., Winter, Y. and Hedenström, A. (2012b). Comparing aerodynamic efficiency in birds and bats suggests better flight performance in birds. *PLoS ONE* **7**, e37335.
Muijres, F. T., Christoffer Johansson, L., Winter, Y. and Hedenström, A. (2014). Leading edge vortices in lesser long-nosed bats occurring at slow but not fast flight speeds. *Bioinspir. Biomim.* **9**, 025006.
Norberg, U. M. (1969). An arrangement giving a stiff leading edge to the hand wing in bats. *J. Mammal.* **50**, 766-770.
Norberg, U. M. (1970). Functional osteology and myology of the wingbeat of *Plecotus auritus* Linnaeus (Chiroptera). *Ark. Zool.* **22**, 485-543.
Norberg, U. M. (1972a). Bat wing structures important for aerodynamics and rigidity (Mammalia, Chiroptera). *Zeitschrift für Morphologie der Tiere* **73**, 45-61.
Norberg, U. M. (1972b). Functional osteology and myology of the wing of the dog-faced bat *Rousettus aegyptiacus* (E. Geoffroy) (Mammalia, Chiroptera). *Zeitschrift für Morphologie der Tiere* **73**, 1-44.
Norberg, U. M. (1976a). Aerodynamics, kinematics, and energetics of horizontal flapping flight in the long-eared bat *Plecotus auritus*. *J. Exp. Biol.* **65**, 179-212.
Norberg, U. M. (1976b). Aerodynamics of hovering flight in the long-eared bat *Plecotus auritus*. *J. Exp. Biol.* **65**, 459-470.
Norberg, U. M. (1981). Allometry of bat wings and legs and comparison with bird wings. *Philos. Trans. R. Soc.* **292**, 359-398.
Norberg, U. M. (1990). *Vertebrate flight. Mechanics, Physiology, Morphology, Ecology and Evolution*. Berlin; Heidelberg; New York, NY: Springer Verlag.
Norberg, U. M. and Rayner, J. M. V. (1987). Ecological morphology and flight in bats (Mammalia; Chiroptera): Wing adaptations, flight performance, foraging strategy and echolocation. *Philos. Trans. R. Soc. B* **316**, 335-427.
Papadimitriou, H. M., Swartz, S. M. and Kunz, T. H. (1996). Ontogenetic and anatomic variation in mineralization of the wing skeleton of the Mexican free-tailed bat, *Tadarida brasiliensis*. *J. Zool.* (*Lond.*) **240**, 411-426.
Pelletier, A. and Mueller, T. J. (2000). Low Reynolds number aerodynamics of low-aspect-ratio, thin/flat/cambered-plate wings. *J. Aircr.* **37**, 825-832.
Pennycuick, C. J. (1971). Gliding flight of the dog-faced bat *Rousettus aegyptiacus* observed in a wind tunnel. *J. Exp. Biol.* **55**, 833-845.
Pennycuick, C. J. (1973). Wing profile shape in a fruit-bat gliding in a wind tunnel determined by photogrammetry. *Period. Biol.* **75**, 77-82.
Pennycuick, C. J. (1975). Mechanics of flight. In *Avian Biology* (ed. D. S. Farner and J. R. King), Vol. 5, pp. 1-75. New York, NY: Academic Press.
Pennycuick, C. J. (1988). On the reconstruction of pterosaurs and their manner of flight, with notes on vortex wakes. *Biol. Rev. Camb. Philos. Soc.* **63**, 299-331.
Pennycuick, C. J. (1989). Span-ratio analysis used to estimate effective lift:drag ratio in the double-crested cormorant *Phalacrocorax auritus* from field observations. *J. Exp. Biol.* **142**, 1-15.
Pennycuick, C. J. (2008). *Modelling the Flying Bird*. Amsterdam: Academic Press.
Pierce, G. W. and Griffin, D. R. (1938). Experimental determination of supersonic notes emitted by bats. *J. Mammal.* **19**, 454-455.
Rayner, J. M. V. (1988). Form and function in avian flight. In *Current Ornithology*, Vol. 5 (ed. R. F. Johnston), pp. 1-66. New York, NY: Plenum Press.
Rayner, J. M. V., Jones, G. and Thomas, A. (1986). Vortex flow visualization reveal change in upstroke function with flight speed in bats. *Nature* **321**, 162-164.
Riskin, D. K., Iriarte-Diaz, J., Middleton, K. M., Breuer, K. S. and Swartz, S. M. (2010). The effect of body size on the wing movements of pteropodid bats, with insights into thrust and lift production. *J. Exp. Biol.* **213**, 4110-4122.
Riskin, D. K., Bergou, A., Breuer, K. S. and Swartz, S. M. (2012). Upstroke wing flexion and the inertial cost of bat flight. *Proc. Biol. Sci.* **279**, 2945-2950.
Rosén, M., Spedding, G. R. and Hedenström, A. (2007). Wake structure and wingbeat kinematics of a house-martin *Delichon urbica*. *J. R. Soc. Interface* **4**, 659-668.
Salehipour, H. and Willis, D. J. (2013). A coupled kinematics-energetics model for predicting energy efficient flapping flight. *J. Theor. Biol.* **318**, 173-196.
Sane, S. P. (2003). The aerodynamics of insect flight. *J. Exp. Biol.* **206**, 4191-4208.
Schnitzler, H.-U. (1971). Fledermause im windkanal. *Z. Vgl. Physiol.* **73**, 209-221.

Shyy, W., Aono, H., Chimakurthi, S. K., Trizila, P., Kang, C.-K., Cesnik, C. E. S. and Liu, H. (2010). Recent progress in flapping wing aerodynamics and aeroelasticity. *Progress in Aerospace Sciences* **46**, 284-327.
Simmons, N. B. (1994). The case for chiropteran monophyly. *Am. Mus. Novit.* **3103**, 1-54.
Simmons, N. B., Seymour, K. L., Habersetzer, J. and Gunnell, G. F. (2008). Primitive early Eocene bat from Wyoming and the evolution of flight and echolocation. *Nature* **451**, 818-821.
Spedding, G. R. (1992). The aerodynamics of flight. In *Advances in Comparative and Environmental Physiology*: *Mechanics of Locomotion*, Vol. 11, (ed. R. McN. Alexander), pp 51-111. Berlin: Springer-Verlag.
Spedding, G. R. and Hedenström, A. (2009). PIV-based investigations of animal flight. *Exp. Fluids* **46**, 749-763.
Spedding, G. R. and McArthur, J. (2010). Span efficiencies of wings at low Reynolds numbers. *J. Aircr.* **47**, 120-128.
Springer, M. S., Teeling, E. C., Madsen, O., Stanhope, M. J. and de Jong, W. W. (2001). Integrated fossil and molecular data reconstruct bat echolocation. *Proc. Natl. Acad. Sci. USA* **98**, 6241-6246.
Sterbing-D'Angelo, S., Chadha, M., Chiu, C., Falk, B., Xian, W., Barcelo, J., Zook, J. M. and Moss, C. F. (2011). Bat wing sensors support flight control. *Proc. Natl. Acad. Sci. USA* **108**, 11291-11296.
Swartz, S. M. (1997). Allometric patterning in the limb skeleton of bats: implications for the mechanics and energetics of powered flight. *J. Morphol.* **234**, 277-294.
Swartz, S. M. and Middleton, K. M. (2008). Biomechanics of the bat limb skeleton: scaling, material properties and mechanics. *Cells Tissues Organs* **187**, 59-84.
Swartz, S. M., Bennett, M. B. and Carrier, D. R. (1992). Wing bone stresses in free flying bats and the evolution of skeletal design for flight. *Nature* **359**, 726-729.
Swartz, S. M., Groves, M. S., Kim, H. D. and Wals, W. R. (1996). Mechanical properties of bat wing membrane skin. *J. Zool. (Lond.)* **239**, 357-378.
Thomas, S. P. (1975). Metabolism during flight in two species of bats, *Phyllostomus hastatus* and *Pteropus gouldii*. *J. Exp. Biol.* **63**, 273-293.
Tobalske, B. W., Warrick, D. R., Clark, C. J., Powers, D. R., Hedrick, T. L., Hyder, G. A. and Biewener, A. A. (2007). Three-dimensional kinematics of hummingbird flight. *J. Exp. Biol.* **210**, 2368-2382.
Usherwood, J. R. and Ellington, C. P. (2002). The aerodynamics of revolving wings I. Model hawkmoth wings. *J. Exp. Biol.* **205**, 1547-1564.
Vaughan, T. A. (1959). Functional morphology of three bats: Bumops, Myotis, Macrotus. *Publ. Univ. Kansas Mus. Nat. Hist.* **12**, 1-153.
Vaughan, T. A. (1966). Morphology and flight characteristics of molossid bats. *J. Mammal.* **47**, 249-260.
Vaughan, T. A. (1970). Flight patterns and aerodynamics. In *Biology of Bats* (ed. W. A. Wimsatt), pp. 195-216. New York, NY: Academic Press.
Viswanath, K., Nagendra,, K., Cotter, J., Frauenthal, M. and Tafti, D. K. (2014). Straight-line climbing flight aerodynamics of a fruit bat. *Phys. Fluids* **26**, 021901.
von Busse, R., Hedenström, A., Winter, Y. and Johansson, L. C. (2012). Kinematics and wing shape across flight speed in the bat, *Leptonycteris yerbabuenae*. *Biol. Open* **1**, 1226-1238.
von Busse, R., Swartz, S. M. and Voigt, C. C. (2013). Flight metabolism in relation to speed in Chiroptera: testing the U-shape paradigm in the short-tailed fruit bat *Carollia perspicillata*. *J. Exp. Biol.* **216**, 2073-2080.
von Busse, R., Waldman, R. M., Swartz, S. M., Voigt, C. C. and Breuer, K. S. (2014). The aerodynamic cost of flight in the short-tailed fruit bat (*Carollia perspicillata*): comparing theory with measurement. *J. R. Soc. Interface* **11**, 20140147.
von Helversen, O. (1986). Blütenbesuch bei blumfledermäusen: kinematik des schwirrfluges und energeibudget in Freiland. In *Bat Flight* (ed. W. Nachtigall), pp. 107-126, Biona Report 5, Stuttgart: G. Fischer.
Warrick, D. R., Tobalske, B. W. and Powers, D. R. (2009). Lift production in the hovering hummingbird. *Proc. Biol. Sci.* **276**, 3747-3752.
Weis-Fogh, T. (1973). Quick estimates of flight fitness in hovering animals, including novel mechanisms for lift production. *J. Exp. Biol.* **59**, 169-230.
Weis-Fogh, T. (1975). Flapping flight and power in birds and insects, conventional and novel mechanisms. In *Swimming and Flying in Nature*, Vol. 2 (ed. T. Y. T. Wu, C. J. Brokaw and C. Brennen), pp. 729-762. New York, NY: Plenum Press.
Wolf, M., Johansson, L. C., von Busse, R., Winter, Y. and Hedenström, A. (2010). Kinematics of flight and the relationship to the vortex wake of a Pallas' long tongued bat (*Glossophaga soricina*). *J. Exp. Biol.* **213**, 2142-2153.
Wolf, M., Ortega-Jimenez, V. M. and Dudley, R. (2013). Structure of the vortex wake in hovering Anna's hummingbirds (*Calypte anna*). *Proc. Biol. Sci.* **280**, 20132391.